B. Billia[1], H. Nguyen Thi[1], G. Reinhart[1], Y. Dabo[1], B.H. Zhou[1,2], Q.S. Liu[2], T.Lyubimova[3], B. Roux[4], C.W. Lan[5]

Tailoring of Dendritic Microstructure in Solidification Processing by Crucible Vibration / Rotation

Directional solidification of alloys, which allows the independent control of growth parameters (pulling velocity, temperature gradient), is an experimental method of choice for the investigation of many fundamental problems (e.g. microstructure formation and selection, segregation of chemical species) encountered in the processing of structural materials. Upward directional solidification is carried out on hypoeutectic Al-Ni alloys, under natural and controlled fluid-flow conditions. First, the influence of natural convection on solidified dendritic microstructure is analyzed as a function of growth parameters. Then, directional solidification experiments with axial vibration are performed. It results that crucible vibration can be used to either damp or control fluid flow in the melt, and thus tailor columnar or "equiaxed" dendritic mush. Advanced modeling and numerical simulation are essential to clarify and quantify the various physical effects. Microgravity benchmark experiments under diffusion transport, and possibly with crucible rotation, are foreseen using the Materials Science Laboratory of ESA on ISS.

Mail Address:

[1)] L2MP, University Aix-Marseille III, Marseille, France

[2)] National Microgravity Laboratory, CAS, Beijing, China

[3)] Institute of Continuous Media Mechanics UB RAS, Perm, Russia

[4)] Laboratoire de Modélisation en Mécanique, Marseille, France

[5)] Department of Chemical Engineering, National Taiwan University, Taiwan

INTRODUCTION

Directional solidification of binary alloys, which allows the independent control of growth parameters (pulling velocity V, temperature gradient G, initial solute concentration C_0), is an experimental method of choice for the investigation of many fundamental problems (e.g. microstructure formation and selection, segregation of chemical species) encountered in the processing of structural materials. Two major features should be noticed. First, solute is rejected in the liquid during the phase transition when the segregation coefficient k is less than unity (k is the ratio of the solute concentration in solid to that in liquid), or rejected when k is higher than unity. Consequently, solidification establishes an exponential solute distribution in the melt which accompanies the thermal profile imposed to drive the growth process. Thus, on Earth, the local liquid density depends on two fields and convection is almost always present in the melt [1]. Second, the planar solid-liquid interface may undergo the Mullins - Sekerka instability [2] which leads to the formation of cells and dendrites. Those patterns are described by shape parameters (primary and secondary spacings, tip radius …) and characteristic relationships have been proposed to relate the shape parameters to the processing conditions when the transport of heat and chemical species is dominated by diffusion [3]. Actually, natural buoyancy-driven convection often plays an important role in terrestrial solidification processing by interacting with the microstructure and modifying the relationships. Moreover, between the fully solid and liquid phases the solid microstructure forms a solid-liquid zone called “mushy zone”, where the phase transition begins and progressively gets complete. For fluid mechanics, this mushy zone can be considered as an intermediate porous medium whose internal structure is composed of fine-scale crystals, through which residual melt flows [4].

In Bridgman solidification, one way to prevent thermosolutal convection is to solidify in a both thermal (i.e. vertical upward solidification) and solutal (i.e. rejected solute denser than sol-

vent) stable configuration. Yet, strong fluid flow driven by radial thermal gradient can be dominant when the growth velocity is slow enough [5]. Then, melt enriched by solute rejection is advected towards the regions of the front where flow is ascending, so that solute concentration is there further enhanced and solidification further retarded. In experiments, the solidification front is generally initially depressed at the periphery of the sample because of the unavoidable radial thermal gradient due to the difference of thermal conductivity between liquid, solid and crucible. Often, the fluid flow adjacent to the solid-liquid interface eventually results in large radial solute segregation concomitant with a radial gradient of microstructure (cells → dendrites → eutectic) as sketched in Fig.1a, which is detrimental to the homogeneity of the grown material. On a longitudinal section, the consequence of this fluid flow is a severe distortion of the solid-liquid interface (Fig.1b), the aluminum cells/dendrites are 'steepled' as their tips protrude markedly into the liquid phase ahead of the eutectic front. Across a transverse section, eutectic growth is visible surrounding the cellular/dendritic cluster. Diffusive-like dendritic growth is achieved beyond a critical pulling rate (Fig.1d). For bulk samples, the most efficient way to obtain diffusion-dominated transport in the melt is to carry out solidification in microgravity environment [6]. On Earth the application of external forces during solidification processing, such as magnetic fields, continuous or alternated rotation around the crucible axis, can be an effective method to control fluid flow in the melt. Indeed, forced convection is commonly used in many crystal growth processes to improve crystal quality such as in Czochralski or floating-zone techniques. In the case of Bridgman solidification, only very few experimental studies [7,8] considered the effects of vibration/rotation on the growth process.

In the present study, attempts are made to analyze experimentally the influence of natural buoyancy-driven convection and of vertical vibration on the solidification microstructure. As the major effect of vibration is to make the surfaces of constant density perpendicular to the vibration direction by altering the temperature and solute fields [9,10], less radial solute segregation and more homogenous microstructures are expected. Solidification experiments with and without vertical vibration were performed on Al - Ni alloy. The influence of the pulling rate on natural convection was first considered. Then, the influence of vertical vibration was investigated by varying the frequency and the amplitude of vibration, for both cellular and dendritic patterns. Finally, advanced modeling and numerical simulation are developed in order to find out the respective roles of the various physical mechanisms into play in the observed phenomena.

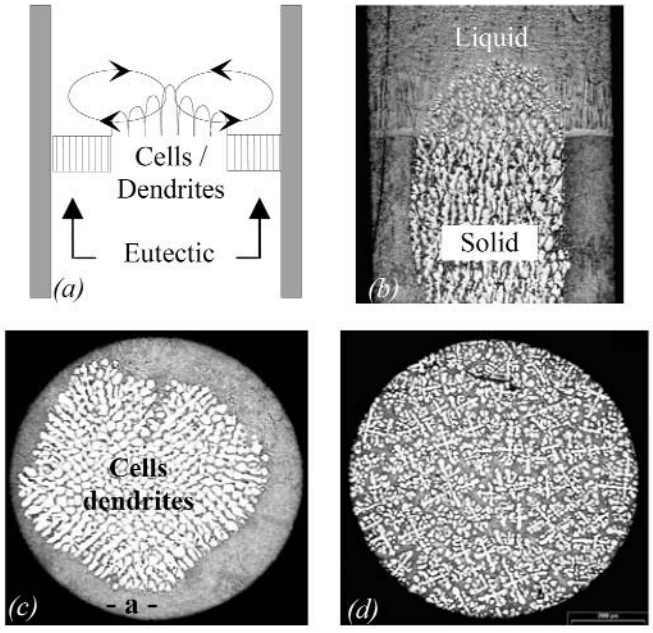

Fig. 1. (a) Sketch of fluid flow driven by the radial thermal gradient, and its distortion effects on the dendritic solidification front. (b) Steepling on longitudinal section and (c) clustering on transverse section at V = 0.7 μm/s. (d) diffusive-like case at V = 9.4 μm/s. Al – 3.5% pds Ni, G = 20 K/cm.

EXPERIMENTAL PROCEDURE

Directional solidification experiments are carried out on Al – 3.5 wt% Ni alloy using a Bridgman-type setup. The furnace, which is fixed, is composed of two independently regulated hot zones and a cooling zone. It is possible to adjust the axial thermal gradient from 20 to 50 K/cm. For the present experiments, the inner tube of the furnace is in alumina, whereas previous similar experiments were carried out with a metallic tube [11].

Each Al - Ni sample, a rod machined to 8 mm in diameter and 110 mm in length, is placed in a boron nitride crucible installed at the top of an alumina rod (20 mm in outer diameter, 650 mm in length) that is moved by a precise translation device. Directional solidification is performed vertically upwards to obtain a thermal and solutal stable configuration. To measure the temperature gradient and the solidification rate during an experiment, the crucible is equipped with four type N thermocouples. An electromagnetic vibrator is mounted at the bottom of the alumina rod, which can apply a longitudinal sinusoidal force to the sample for a wide range of frequency f (10 - 50 Hz) and amplitude α (0.25 – 1.25 mm) to get various values of

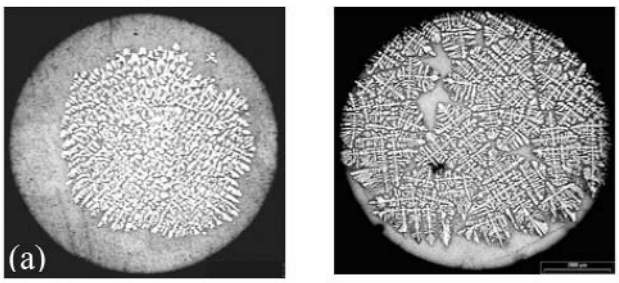

Fig. 2. Solidification microstructures under natural convection : (a) Cellular, V = 1.0 μm/s, (b) Dendritic, V = 7.2 μm/s. Al – 3.5 wt% Ni, G = 30 K/cm. No vibration.

vibrational acceleration $g_{vib} = a\ (2\ \pi f)^2$. It is worth noticing that the vibrations are applied during thermal stabilization, fifteen minutes before the start of pulling, and during solidification processing.

Experiments are carried out under an argon atmosphere. After a solidified length of typically 30 mm, steady-state conditions are reached and the remaining liquid is quenched by a rapid furnace displacement to freeze the interface microstructure, which is later analyzed by metallography in both transverse and longitudinal sections cut in the stationary part of the sample. Then, both sections are mechanically polished until the cells, or dendrites, appear. There is no need of chemical etching since primary aluminum phase Al_3Ni phase give enough contrast for optical observation.

EFFECT OF NATURAL CONVECTION

Increasing the solidification rate within the range 0.1–30 μm/s, eutectic, cellular and dendritic microstructures are observed for Al - 3.5 wt % Ni alloy solidified in an almost constant thermal gradient G = 30 K/cm (Fig.2). First, at very low growth rate (V = 0.1 μm/s) a planar eutectic front is obtained and no marked effect of convection is visible. Then, for V = 0.3-1.0 μm/s, the solidification front is cellular and there is a strong effect of convection, which again generates the clustering and steepling phenomena previously described (Fig.2a). The cross section shows that, all around dendrite clusters, the dendrites arms are growing horizontally towards the surrounding eutectic. Increasing further the solidification rate (Fig.2b), the dendritic microstructure becomes more and more ramified and the clustering effect of convection progressively decreases (i.e. the eutectic border progressively disappears). For still higher pulling rate, an almost homogeneous pattern is observed in cross section as in Fig.1d. The transition from a strongly disturbed dendritic microstructure to an almost homogeneous pattern can be estimated to occur at a solidification rate V in between 16 and 24 μm/s. For the previous experiments described in [11] performed with a metallic tube, the transition occurred at about 10 μm/s, which points out the critical role played by the heat transfer on this type of convection. Besides, experiments with another concentration (Al-1.5 wt% Ni) and/or various thermal gradients (20 and 50 K/cm) gave the same general features [11]. Our experimental results further validate the microstructure evolution predicted by Dupouy *et al* [12], with a critical velocity beyond which solidification produces a uniform diffusion-like array of dendrites.

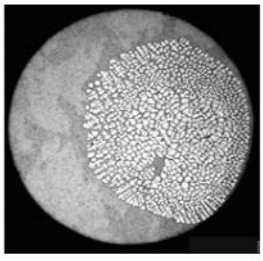

Fig. 3. Solidification microstructure for (a) no vibration,(b) $g_{vib} = 2.5g_0$ (f = 50 Hz, a = 0.25 mm). Al – 3.5 wt% Ni alloy, G = 30K/cm, V = 1.0 μm/s.

INFLUENCE OF VIBRATIONS

To examine the effects of longitudinal sinusoidal vibration on directional solidification, four series of experiments are carried out for Al - 3.5 wt % Ni alloy with the same thermal gradient (30 K/cm) for different pulling rates V = 1 – 3 – 7.2 - 9 μm/s. The solidification microstructure evolves from a cellular pattern to a dendritic pattern, which correspond respectively to a shallow mushy zone with small liquid fraction and a deep mushy zone with large liquid fraction. For each series of experiments, the influence of the vibration level on the microstructure is analyzed as a function of the vibration frequency and amplitude. The experimental results show that the changes induced by vibration on the solidification morphology strongly depend not only on the vibration acceleration, but also on the type of microstructure (cellular or dendritic). In the following, the discussion is restricted to V = 1 μm/s and 7.2 μm/s.

Cellular growth

For cellular growth (V = 1 μm/s), very limited changes are induced by axial vibration as shown in Fig.3, regardless of the vibration acceleration g_{vib} ($g_{vib} = a\ (2\ \pi f)^2$ and $g_{vib} = 0$ is the natural convective situation). This is probably due to the lack of

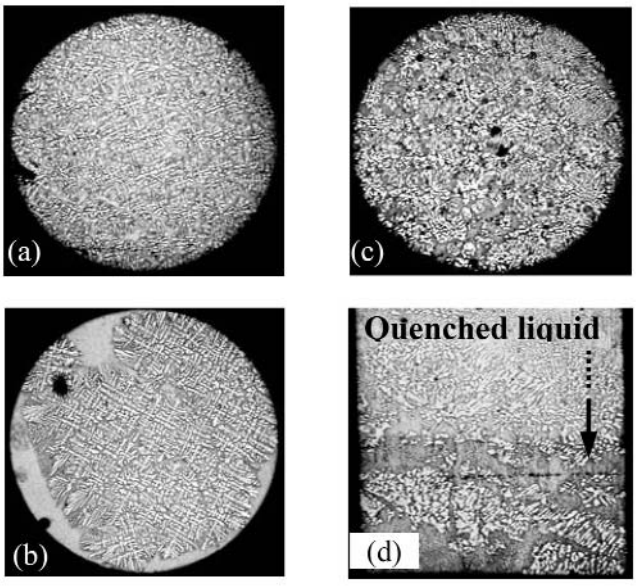

Fig. 4. (a, b) Solidification microstructure for two sets of vibration parameters giving the same $g_{vib} = 1.0g_0$: (a) f = 14 Hz, a = 1.25 mm, (b) f = 16 Hz, a = 1.0 mm. (c,d) Cross and longitudinal sections showing the solidification microstructure for $g_{vib} = 2.5g_0$, f = 50 Hz, a = 0.25 mm. Al – 3.5 wt% Ni, G = 30K/cm. V = 7.2 μm/s.

porosity of the mushy zone. Indeed, the liquid fraction at the interface is very low and fluid flow cannot go deep into the mush. Fluid flow cannot develop on a large scale in the interior of the mushy zone and remains mainly parallel to the mush-liquid interface [6]. Therefore, the influence of natural and forced convection on the average primary spacing of the cellular array ($\lambda_{conv} \approx$ 200-300 μm in the core of the cell cluster) is expected to be rather weak. The main effect of vibration is to push the cellular area on one side of the transverse section. This suggests that vibrations may be either not perfectly axial or break the fluid-flow mode of natural buoyancy convection. Further experiments or numerical simulations are required to give a definitive answer to this observation.

Dendritic growth

For dendritic growth (V = 7.2 μm/s), experiments with vibration acceleration g_{vib} varied from $0.5g_0$ to $2.5g_0$ are carried out. For the lowest value of g_{vib}, the microstructure is very similar to the case of natural convection (Fig.2b). Then, axial vibrations induce neat changes, in particular finer solidification microstructures. When the vibrational acceleration is about $1.0g_0$, two different cases are obtained, depending on the value of the vibration amplitude and frequency. For a = 1.25 mm and f = 14 Hz, the morphology becomes more homogeneous with almost no eutectic border (Fig.4a) whereas the microstructure is still strongly disturbed by convection for a = 1.0 mm and f = 16 Hz (Fig.4b). This suggests that the effect of vibrations must be characterized not only by g_{vib} but also by a and f separately. The behavior is quite different for higher levels of vibration, e.g. at $2.5g_0$ (f = 50 Hz, a = 0.25 mm), the dendritic morphology is fragmented and a great number of somewhat globular clusters of cells or dendrites are distributed in a cross section (Fig.4c). The longitudinal section reveals a pattern resembling equiaxed growth (Fig.4d). Presently, it is difficult to decide whether or not some secondary arms are detached from primary stems during the growth process, which is a key question for the columnar to equiaxed transition in materials processing.

MODELING AND NUMERICAL SIMULATION

From the previous experimental observations, it is obvious that the coupling between heat and solute transport, hydrodynamics and solidification is both very subtle and intricate so that recourse to advanced modeling and numerical simulation is mandatory to clarify the role of the physical mechanisms that are into play. For the mere sake of tractability, our strategy at start is to split the general problem into two simpler cases, one fully rigorous but ignoring the solidification microstructure and the other including a phenomenological model of the mush. Both approaches take into account the liquid, the solid, the moving interface and the crucible.

On the one hand, a numerical algorithm has been developed to perform fully time-dependent direct numerical simulation of flows and heat and mass transfer during directional solidification in a cylinder without and with buoyancy-driven or/and vibration/rotation-forced fluid flow [9], in the Boussinesq approximation and in the limit of a smooth solid-liquid interface (Fig.5). It follows that the intensity of the flow induced by axial vibration is low in comparison with the buoyancy-driven flow (Fig.5a,b). Conversely, rotational vibrations at f = 10Hz with angular amplitude α = 0.0025 rd generate a counter-rotating flow at the solidification front so that the natural-convection vortex is screened (Fig.5c) and the isoconcentration lines are flattened in the lower part of the melt (Fig.5d).

On the other hand, to understand the physical contribution coming from the mushy zone an axisymmetric model based on a stream function/vorticity formulation and finite volume method is used [13]. The heating profile is described by a hyperbolic tangent function fitted to the measured one. A criterion for microstructure selection between dendrites and eutectic is embedded in the code. Namely, dendrites win as long as the tip temperature is greater than the eutectic temperature. As the mushy zone, that can be viewed as the consequence of morphological instability, acts to reduce the region of constitutional supercooling in the system, we adopt here the suggestion of Worster et al. [4] of marginal equilibrium condition at the mush-

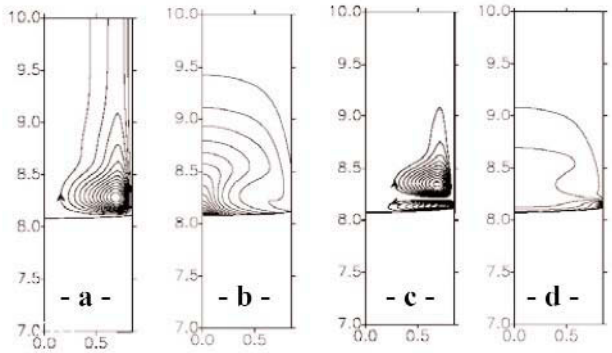

Fig. 5. Fluid flow and solute field for (a,b) natural buoyancy-driven convection and (c,d) rotational vibration. Model alloy system: succinonitrile – 2.6x10^{-3} wt% ethanol, V = 1 μm/s, G = 10 K/cm.

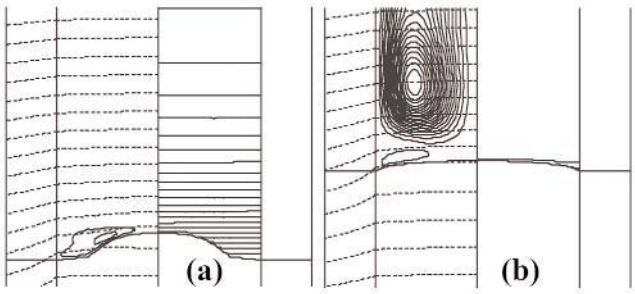

Fig. 6. Numerical results for solidification rate V = (a) 0.7μm/s; (b) 9.4μm/s. Streamlines and isotherms (dashed lines) on the left, solute field on the right. Al – 3.5wt% Ni, G = 20 K/cm.

liquid interface, where zero flow velocity is assumed. In other words, the normal temperature gradient at the mush-liquid interface is equal to the normal gradient of equilibrium temperature.

The numerical results of numerical simulations with only buoyancy-driven fluid flow are summarized in Fig.6 for V = 0.7 and 9.4 μm/s. Those results are sufficient to explain the evolution in steepling and clustering phenomena reported in Fig.1. The temperature and solute distributions, and flow field for V = 0.7μm/s are shown in Fig.6a. The interface shape departs from an isotherm and dendrites protrude into the melt. Due to the thermal mismatch between the hot and adiabatic zones, a large convective cell (not shown) is formed in the bulk liquid. Because the rejected solute is denser, the convection near the liquid-mush/eutectic interface driven by the radial thermal gradient remains confined to the solute boundary layer. Thus, no longitudinal macrosegragation happens and steady growth can be reached, in agreement with the experimental results. Fluid flow near the liquid-mush/ eutectic interface is descending in the center, which decreases the thickness of solute boundary layer, an ascending on the periphery with the opposite effect. Then, the solute gradient is augmented in the center, which promotes morphological instability there. On the contrary, the solute gradient is reduced on the periphery, where the breakdown of the eutectic front is retarded. For V = 9.4μm/s, the overall interface becomes slightly convex and is composed of liquid/mush interface only (Fig.6b), as in Fig.1d where only dendrites are observed. The upper convective cell has now invaded the bulk melt, while remaining not felt by the liquid/mush interface for the same reason as before so that there is still no longitudinal macrosegregation. It is worth noticing the difference with Fig.5a,b where ethanol is a light solute.

Finally, preliminary results with continuous crucible rotation at frequency Ω are given in Fig.7. Due to the centrifugal force with acceleration $r\Omega^2$, where r is the radial coordinate, the bulk convection now cooperatively couples with fluid flow in the solute boundary layer which deforms the isoconcentration lines. This effect is opposite to that of rotational vibration in Fig.5c,d, which confirms that the predictions of sound modeling and numerical simulations are precious for the clever choice of vibration parameters in experiments.

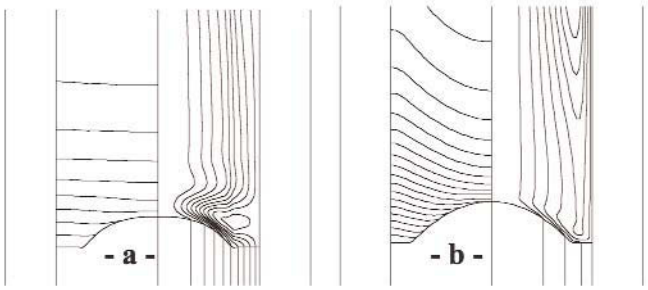

Fig. 7. Effect of crucible rotation at 200 RPM on solute field (left) and streamlines (right) and on clustering (b) compared to natural convection case (a). Al – 3.5 wt% Ni, V = 1 μm/s, G = 20 K/cm.

CONCLUSION

Directional solidification experiments are carried out under natural and vibration-controlled conditions. The role of processing parameters (pulling rate and vibration level) is systematically evaluated. The experimental results provide evidence that axial vibration of the crucible can strongly modify fluid flow in the melt and thus act on the solidification microstructure. The response of the solidification front depends on the growth microstructure, the effects being more pronounced for dendritic patterns when there is a deep mushy zone. When the vibration level is above $2g_0$, the microstructure becomes fragmented, somewhat equiaxed, and columnar growth is suppressed. To guide the experiments and deepen the understanding, companion advanced modeling and numerical simulations have been started. Although illuminating, the first results stress the complexity of the couplings between the basic physical phenomena so that complementary work is in progress.

ACKNOWLEDGMENTS

Support of ESA (CETSOL MAP) and CNES (GDR Phénomènes de Transport et Transitions de Phases en Micropesanteur) is gratefully acknowledged.

REFERENCES

[1] *Davis, S.H.*, J. Fluid Mech., vol. 212, p. 241 (1990).
[2] *Mullins, W.W., Sekerka, R.F.*, J. Appl. Phys., vol. 35, p. 444 (1964).
[3] *Hunt, J.D., Lu, S.Z.*, Metall. Mater. Trans. A, vol. 27, p. 611 (1996).
[4] *Worster, M.G.*, J. Fluid Mech., vol. 237, p. 649 (1992).
[5] *Burden, M.H., Hebditch, D.J. Hunt, J.D.*, J. Cryst. Growth, vol. 20, p. 121 (1973).
[6] *Drevet, B., Nguyen Thi, H., Camel, D., Billia, B., Dupouy, M. D.*, J. Crystal Growth, vol. 218, p. 419 (2000).
[7] *Sarkar, S., Banerjee, M.K., Seal, A.K.*, vol. 38, p. 139 (1985).
[8] *Grugel, R.N., Kim, S., Woodward, T., Wang, T.G.*, J. Crystal Growth, vol. 121, p. 599 (1992).
[9] *Gershuni, G.Z., Lyubimov, D.V.*: Thermal Vibrational Convection. Wiley, New York, (1998).
[10] *Savino, R., Monti, R.*, Int. J. Heat Mass Transfer, vol. 42, p. 111 (1999).
[11] *Zhou, B.H.*, et al., in : Proc. Int. Conf. "Advanced Problems in Thermal Convection". Lyubimova T. (Ed), to appear.
[12] *Dupouy, M.D., Camel, D.*, J. Crystal Growth, vol. 183, p. 469 (1998).
[13] *Lan, C.W., Tu, C.Y.*, J. Crystal Growth, vol. 220, p. 619 (2000).